On the Synthesis of Stable Switching Dynamics to Approximate Limit Cycles of Nonlinear Oscillators

Nils Hanke ^{©a}, Zonglin Liu ^{©b} and Olaf Stursberg ^{©c} Control and System Theory, EECS Dept., University of Kassel, Germany

Keywords: Oscillators, Limit Cycles, Approximation, Switching Affine Systems, Stability.

Abstract:

This paper presents a novel method for approximating periodic behavior of nonlinear systems by use of switching affine dynamics. While previous work on approximating limit cycles by switching systems has been restricted to state space partitions with only two regions or approximations in the plane, this study employs more general partitions in higher-dimensional spaces as well as external signals to develop a scheme for synthesizing models with guaranteed existence of a globally stable limit cycle. The synthesis approach is formulated as a constrained numeric optimization problem, starting from sampled nonlinear dynamics data. It minimizes deviations between this data and the switching affine model's limit cycle, while satisfying constraints to ensure global stability. The principle and effectiveness of the proposed method is illustrated through examples.

1 INTRODUCTION

Periodic behavior is a fundamental phenomenon observed across numerous application domains, including biology, engineering, and physics (Teplinsky and Feely, 2008; Mirollo and Strogatz, 1990; Peterchev and Sanders, 2003). While nonlinear oscillator models such as Kuramoto, Van-der-Pol, FitzHugh-Nagumo, Duffing, or Goodwin oscillators (Kuramoto, 2005; Joshi et al., 2016; Gaiko, 2011; Dörfler and Bullo, 2014; Kudryashov, 2021; Gonze and Ruoff, 2021; Atherton and Dorrah, 1980) are widely used to describe periodic behavior, the analysis of these models is limited: Specifically, the characterization and analysis of limit cycles, including conditions for uniqueness and stability, is often restricted to special cases. A central challenge in studying such behavior is to approximate the underlying oscillatory dynamics with an analytically tractable system class which allows to rigorously analyze its properties. Existing data-driven approaches, such as machine learning or hybrid system identification, can approximate periodic behavior (Xu and Luo, 2019), but they are not designed to allow for rigorous analysis of properties of limit cycles. This gap hinders the systematic study of oscillatory phenomena in applications such as, e.g., the investigation of circadian rhythms in biological systems (Werckenthin et al., 2020), where un-

a https://orcid.org/0009-0008-8940-2677

derstanding stability, phase shifts, and synchronization is essential.

To simplify the model analysis, switching or piecewise-affine systems (PAS) have proven effective in approximating nonlinear dynamics (Paoletti et al., 2007; Lauer et al., 2011). This is primarily due to the facts that (1.) the analytic solution of piecewiseaffine systems exists for each region of the partitioned state space, and (2.) the approximation quality can be tuned through adapting the partitioning and parametrization. Specifically with respect to the approximation of nonlinear systems with periodic trajectories, the work in (Lum and Chua, 1991; Freire et al., 1998) proposed conditions for the existence of limit cycles of PAS (with two-region partitions) in \mathbb{R}^2 . The uniqueness and stability of these limit cycles are further examined in (Coll et al., 2001; Llibre et al., 2008). These results are then adopted in (Kai and Masuda, 2012) to synthesize PAS with stable limit cycles in \mathbb{R}^2 , while the work in (Hanke and Stursberg, 2023; Hanke et al., 2024) further developed algorithms to generate planar switching affine systems to approximate given limit cycles with guarantees of uniqueness and local stability. However, there the use of only two affine dynamics and a single separating line limits the approximation quality. A comprehensive review of the conditions of the existence of limit cycles in planar piecewise-linear systems can be found in (Freire et al., 1998) or in Chapter 5.1 of (Bernardo et al., 2008). The recent work (Hanke et al., 2025) improved the approximation quality by employing multiple partitions, however the proposed result is still limited to

b https://orcid.org/0000-0002-0196-9476

^c https://orcid.org/0000-0002-9600-457X

the \mathbb{R}^2 , and it lacks the guarantee of global stability of the limit cycle.

This paper extends the approaches in literature to higher-dimensional spaces by leveraging the contraction property outlined in (Pavlov et al., 2007) to generate PAS with globally stable limit cycles. A novel method is proposed for partitioning the state space and synthesizing affine dynamics within each region, ensuring both global stability and adjustable approximation quality.

Section 2 first introduces properties of PAS which are essential for ensuring high approximation quality. Section 3 proposes rules for partitioning state spaces of arbitrary dimensions and for synthesizing PAS with desired properties by use of optimization. An illustrative numerical example is presented in Sec. 4, including cases in 2 and 3 dimensions, before conclusions and an outlook are provided in Sec. 5.

2 PROBLEM DESCRIPTION

The objective of the procedure to be proposed in this paper is to reconstruct limit cycles of a broad class of oscillatory systems with the following property: The underlying nonlinear dynamics (defined in \mathbb{R}^{n_x}) generates a smooth and stable limit cycle which 1.) is embedded in an $(n_x - 1)$ -dim. manifold, 2.) oscillates around a virtual center point, and 3.) does not show strong twisting nor points of intersection with itself.

Assume that an ordered set $F := \{\tilde{x}_1, \tilde{x}_2, \dots, \tilde{x}_{n_F}\}$ of different state samples $\tilde{x}_i \in \mathbb{R}^{n_x}$ is taken along the limit cycle of the nonlinear dynamics. For the sake of clarity, it is assumed that the sampling time Δt is constant along the cycle, while the method introduced later is also applicable to cases with nonuniform sampling times. The sampling is assumed to be dense in the sense that n_F is much larger than n_x , i.e., the sampling time Δt is much smaller than the period $T = n_F \cdot \Delta t$ of the limit cycle, and $\Delta t < 1$ applies.

Given F, the objective of this paper is to propose a method to construct a dynamic model approximating the limit cycle of the nonlinear dynamics while preserving its properties – for this purpose, the class of switching affine systems is chosen: Let $x(t) \in \mathbb{R}^{n_x}$ denote the state at time $t \in \mathbb{R}$ and $u(t) \in \mathbb{R}$ a scalar input signal, which is multiplied by a vector $B \in \mathbb{R}^{n_x \times 1}$. Assume that the state space \mathbb{R}^{n_x} is partitioned into finitely many polytopes $P_i \subseteq \mathbb{R}^{n_x}$, $i \in \{1, \dots, n_P\}$, which are parametrized by $C_i \in \mathbb{R}^{1 \times n_x}$, $d_i \in \mathbb{R}$, and $C_{n_P+1} = C_1$, $d_{n_P+1} = d_1$ according to:

$$P_{i} := \{x \in \mathbb{R}^{n_{x}} | C_{i}x \ge d_{i}, C_{i+1}x < d_{i+1}\}, \bigcup_{i=1}^{n_{P}} P_{i} = \mathbb{R}^{n_{x}}. \quad (1)$$

Note that this definition is particular in the sense that the number of P_i and bounding planes (C_i, d_i) is both n_p , as required for the procedure to be proposed. For pairs (A_i, b_i) of $A_i \in \mathbb{R}^{n_x \times n_x}$ and $b_i \in \mathbb{R}^{n_x \times 1}$, the affine dynamics assigned to each P_i is:

 $\dot{x}(t) = A_i x(t) + b_i + Bu(t)$, for $x(t) \in P_i$. (2) Consider a set of switching times $T_k = \{t_0, t_1, \ldots\}$ with the initial time $t_0 = 0$. A trajectory $\bar{x}_{[0,\infty[}$ of (2), starting from the initial state $x(t_0) = x_0$, contains the state evolution for a sequence of phases $[t_k, t_{k+1}]$ in between two successive switching times. In each phase with $t \in [t_k, t_{k+1}]$, the pair (A_i, b_i) in (2) is activated for the index i for which $x(t) \in P_i$ applies. A limit cycle, as a

Definition 1. Limit Cycle

A trajectory $\bar{x}_{[0,\infty[}^*$ of (2) is called limit cycle, if a finite period $T \in \mathbb{R}_{>0}$ exists such that for any point $x(t) \in \bar{x}_{[0,\infty[}^*$, $t \in \mathbb{R}_{\geq 0}$ it applies that: x(t+T) = x(t).

particular trajectory of (2), is defined as follows:

Definition 2. Stability of a Limit Cycle

A limit cycle $\bar{x}_{[0,\infty[}^*$ of (2) is called globally stable, if every trajectory converges towards $\bar{x}_{[0,\infty[}^*$ independent of the initialization $x(0) = x_0 \in \mathbb{R}^2$.

The identification of a model of type (2) from F requires to synthesize the following parameters: 1.) the number n_P of elements P_i of the state space partition, 2.) the boundaries $C_i x = d_i$ of the P_i , 3.) the pair of matrices (A_i, b_i) for each P_i , and 4.) the signal u(t) together with the vector B. To match the properties assumed for the limit cycle of the nonlinear system, the particular synthesis requirements are:

- The evolution of (2) also forms a limit cycle x̄^{*}_{[0,∞[}, which is globally stable according to Def. 2.
- The period of the limit cycle $\bar{x}_{[0,\infty]}^*$ is $T = n_F \cdot \Delta t$.
- The limit cycle $\bar{x}_{[0,\infty[}^*$ tracks the sample points in F as well as possible.

Switching affine systems are a promising candidate for such an approximation, since the number of parameters in each P_i is small and the dynamics is relatively simple to analyze. In particular, if the considered dynamics is strongly nonlinear along the cycle, the approximation with affine dynamics in restricted regions is well justified, while freedom in choosing the P_i (wrt. number and positioning) allows in principle to obtain arbitrarily good approximations. However, most existing work on approximating limit cycles is limited to either two regions in the plane, or provides only local stability guarantees. To address these limitations, the following exposition uses the concept of contractivity to obtain a synthesis procedure achieving the named properties of $\bar{x}_{[0,\infty[}^*$ by numerical optimization.

3 SYNTHESIS OF CONTRACTIVE SWITCHING AFFINE SYSTEMS

3.1 Partitioning of the State Space

In order to fully utilize the degrees of freedom offered by (2) in assigning different affine dynamics to the regions when tracking the set of samples $F := \{\tilde{x}_1, \tilde{x}_2, \dots, \tilde{x}_{n_F}\}$, a method for partitioning the state space in any dimension $n_p \in [2, n_F - 1]$ is introduced first. This method ensures that the resulting partition satisfies the conditions in (1). Specifically, the cases of $n_x = 2$, $n_x = 3$, and $n_x > 3$ are discussed separately in the sequel.

Case $n_x = 2$: Let a *center point* x_s of all points in F be determined by:

$$x_{s,[q]} = \frac{1}{2} \left(\max_{l \in \{1,\dots,n_F\}} \tilde{x}_{l,[q]} - \min_{l \in \{1,\dots,n_F\}} \tilde{x}_{l,[q]} \right)$$
(3)

for both dimensions $q \in \{1,2\}$. By assuming that x_s does not coincide with any point in F, a set of n_p sample points $\hat{x}_1, \dots, \hat{x}_{n_p}$ is selected from F, see Remark 2 at the end of this subsection for more details. Then, for each point \hat{x}_i , a unique line $C_i x = d_i$ with $C_i \in \mathbb{R}^{1 \times 2}$, $d_i \in \mathbb{R}$, can be determined, which contains x_s and \hat{x}_i . Such a line then serves as the boundary between the regions P_{i-1} and P_i , as illustrated in Fig. 1.

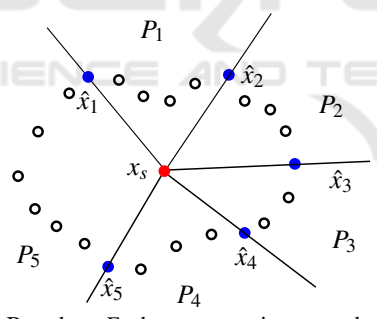


Figure 1: Based on F, the center point x_s , and a set of selected points $\hat{x}_1, \dots, \hat{x}_{n_P} \in F$ (each representing the first state of any subset F_1, \dots, F_{n_P} along the limit cycle), the lines for partitioning X into regions P_i are determined.

Case $n_x = 3$: Let the center point x_s again be determined by (3). Then, a plane $\Omega^* x = \varepsilon^*$ with $\Omega^* \in \mathbb{R}^{1 \times 3}$, $\varepsilon^* \in \mathbb{R}$, is determined by:

$$(\Omega^*, \varepsilon^*) := \underset{\Omega, \varepsilon}{\arg\min} \sum_{i=1}^{n_F} \|\Omega \tilde{x}_i - \varepsilon\|_2, \text{ s.t. } \Omega x_s = \varepsilon \quad (4)$$

Based on the outcome of (4), a line:

$$\Gamma := \{ x \in \mathbb{R}^3 \mid x = x_s + \eta \Omega^*, \ \eta \in \mathbb{R} \}$$
 (5)

which contains x_s and shares the direction vector Ω^* is obtained. Note that the plane $\Omega^* x = \varepsilon^*$ contains the

center point x_s , while the overall distance between the sample points in F to the plane is minimized across all possible values of Ω and ε . If no point in F is contained in Γ , a set of n_p sample points $\hat{x}_1, \ldots, \hat{x}_{n_p}$ is selected from F. For each of these sample points \hat{x}_i , a unique plane containing \hat{x}_i and the line Γ is determined. If such a plane does not contain any other sample point from F, then it is assumed to constitute the boundary $R_{i-1,i} := \{x \in \mathbb{R}^3 | C_i x = d_i\}$ between two adjacent regions P_{i-1} and P_i . In this way, a partition which does not satisfy (1), as illustrated in Fig. 2a), is avoided. An admissible partitioning from the aforementioned procedure is shown in Fig. 2b).

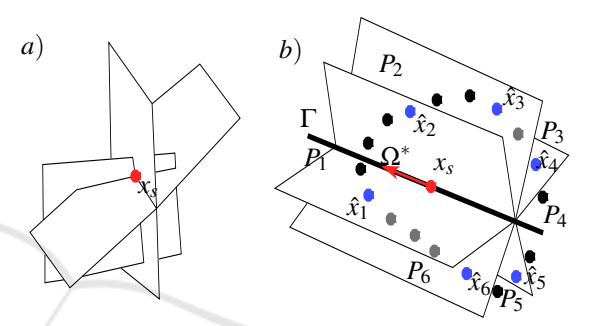


Figure 2: For $n_x = 3$, the partitioning shown in Fig. 2 a) does not satisfy (1). In contrast, an admissible partition is obtained by the considered procedure for the case in Fig. 2 b).

Case $n_x > 3$: Determine again x_s , the vector $\Omega^* \in \mathbb{R}^{1 \times n_x}$, and the line Γ according to (3) to (5). Let also n_p sample points $\hat{x}_1, \ldots, \hat{x}_{n_p}$ be selected from F. However, for any of these sample points \hat{x}_i , a hyperplane containing \hat{x}_i and the line Γ (while being defined in an $n_x - 1$ dimensional subspace) is not unique. To resolve this issue, a set of linearly independent vectors $\Omega_2, \ldots, \Omega_{n_x-2}, \Omega_j \in \mathbb{R}^{1 \times n_x}$, are identified, which have to be linearly independent of Ω^* . Based on these vectors, a hyperplane Ψ can be determined in the $n_x - 2$ dimensional subspace by:

$$\Psi := \{ x \in \mathbb{R}^{n_x} | x = x_s + \eta_1 \Omega^* + \sum_{j=2}^{n_x - 2} \eta_j \Omega_j, \ \eta_j \in \mathbb{R} \}.$$
 (6)

Assume that Ψ does not contain any points from F, then for each sample point \hat{x}_i , a unique hyperplane in the n_x-1 dimensional subspace can be determined, which contains Ψ and \hat{x}_i . If such hyperplane does not contain any other sample point from F, this hyperplane is then chosen to be the boundary $R_{i-1,i} := \{x \in \mathbb{R}^{n_x} | C_i x = d_i\}$ between the regions P_{i-1} and P_i .

Remark 1. The proposed procedure a-priori excludes sets F that are likely to yield poor approxi-

 $^{^{1}}If$ this condition does not hold, one may resolve the issue by slightly changing $\Omega^{\ast}.$

mations. One of these cases is shown in Fig. 3 a), in which the condition is not satisfied that $C_i x = d_i$ does only contain one sample point \hat{x}_i and one line Γ . The second case, shown in Fig. 3 b), corresponds to a limit cycle intersecting itself. While the proposed partitioning procedure may succeed here, it becomes clearly evident, e.g. for P_3 , that no affine system can be found that adequately captures the opposing directions of motion of the trajectories. This limitation motivates the exclusion of limit cycles with intersections, as stated in Sec. 2.

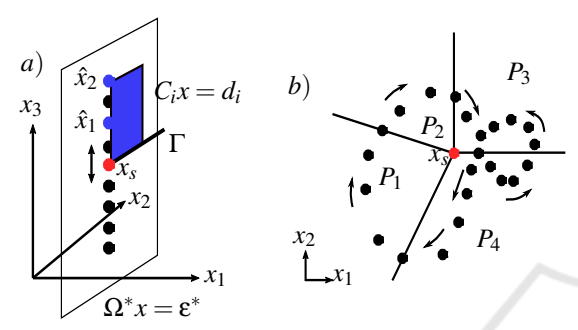


Figure 3: Types of sets F that are not suitable for the partitioning procedure under consideration: the case in a) fails to meet the condition that $C_i x = d_i$ does only contain a sample point \hat{x}_i and Γ , while the case in b) is not feasible for determination of $A_3, b_3 \in P_3$ and $A_4, b_4 \in P_4$.

Remark 2. The n_p sample points of the sequence $\{\hat{x}_i\}_{i=1}^{n_p}$ with timestamps $\{\hat{t}_i\}_{i=1}^{n_p}$ are selected from F such that all time intervals satisfy:

$$\Delta \hat{t}_i := |\hat{t}_{i+1} - \hat{t}_i| < 1 \quad \forall i \in \{1, \dots, n_p\}$$
 (7)

with $\hat{t}_{n_p+1} \equiv t_1$. While this selection is not strictly necessary to partition the state space, it enables good approximation quality in the reconstructed limit cycle, as will be discussed in Sec. 3.3.

3.2 Construction of the Dynamics

Assume that the number n_F and the partition (1) into P_i are fixed. According to (Pavlov et al., 2007), the switching affine system (2) is said to be *contractive*, if the following is satisfied:

- Condition 1: $A_ix + b_i = A_{i+1}x + b_{i+1}$ holds for all x on the boundary $C_ix = d_i$ and for all $i \in \{1, ..., n_P\}$, with $A_{n_p+1} = A_1$ and $b_{n_p+1} = b_1$.
- Condition 2: $A_i^T Q + QA_i \prec 0$ holds for all $i \in \{1, ..., n_P\}$ with a positive-definite matrix $Q \succ 0$.

The first condition requires that the gradient of the autonomous dynamics on the switching boundaries must be continuous, while the second condition implies the existence of a common Lyapunov function in all regions. Next, the important property of contractivity is established, which underlies the synthesis procedure in this paper:

Lemma 1. (Contractive switching affine systems (Demidovich, 1967; Pavlov et al., 2007)) If the system (2) is contractive with a non-zero vector B, then for any piecewise continuous periodic signal u(t) with a period T, the solution x(t), $t \ge 0$ starting from an arbitrary $x(0) \in \mathbb{R}^{n_x}$ always converges to a unique limit cycle with the same period T.

In order to encode the requirement of continuous gradients on the switching boundaries, the following equality constraints for synthesizing (A_i,b_i) , $i \in \{1,\ldots,n_P\}$ are proposed:

$$A_{i,[q]} - A_{i+1,[q]} = \alpha_{i,[q]} C_i, \ b_{i,[q]} - b_{i+1,[q]} = \alpha_{i,[q]} d_i$$
 (8)

for $\alpha_{i,[q]} \in \mathbb{R}$ and $q \in \{1,\ldots,n_x\}$, where $A_{i,[q]}$ represents the q-th row of A_i .

The condition for the existence of a common Lyapunov function represents a nonlinear matrix inequality involving the matrices A_1, \ldots, A_{n_P} and Q. If these constraints are satisfied, the system (2) is ensured to have a globally stable limit cycle as in Def.s 1 and 2 with a period of T (provided that the signal u(t) is also periodic with the same length, see Lemma 1). The task is thus to adapt (2) in order to achieve that the limit cycle approximates the sample points in F with respect to position and time.

3.3 Tracking the Sample Points in *F*

For tracking the sample points in a set F_i , consider the set F_1 explicitly – the following procedure can then be transferred to the other sets F_i , $i \in \{2, ..., n_P\}$ equivalently. For $F_1 = \{\hat{x}_1, \tilde{x}_2, ..., \tilde{x}_{n_1}\}$ with n_1 denoting the number of points in F_1 and $\hat{x}_1 = \tilde{x}_1$, the following cost functional is defined:

$$J_{1} := \sum_{j=2}^{n_{1}} ||e^{A_{1}(j-1)\Delta t} \hat{x}_{1} + \dots$$

$$\int_{0}^{(j-1)\Delta t} e^{A_{1}((j-1)\Delta t - \tau)} (b_{1} + Bu(\tau)) d\tau - \tilde{x}_{j}||_{2}^{2}. \quad (9)$$

It records the difference between the reachable points of $\dot{x}(t) = A_1 x(t) + b_1 + B u(t)$ (starting from \hat{x}_1) and the sampled points in F_1 at each sampling time².

By synthesizing A_1 , b_1 and B for a given signal u(t), the first challenge in minimizing J_1 is the nonlinearity caused by the matrix exponential function e^{A_1t} .

 $^{^2}$ For sampled states in F with non-uniform but known sampling times, only the corresponding times in (9) need to be adjusted.

Based on the Taylor series:

$$e^{A_1t} = I_{n_x} + A_1t + \frac{1}{2!}A_1^2t^2 + \dots \approx I_{n_x} + \sum_{i=1}^{n_d} \frac{1}{j!}A_1^jt^j$$
 (10)

the value of e^{A_1t} can be approximated by the righthand side of (10) with sufficiently high order n_d . If the state dimension n_x is large, a high order n_d would increase the complexity of the optimization significantly (due to a higher-order nonlinearity), whereas a smaller order (such as $n_d \le 3$) would lead to a nonnegligible approximation error. To this end, two possible countermeasures are introduced:

- For a fixed matrix A₁, the approximation error in (9) is small for small times t. Especially for t < 1 the series t^j, j ∈ {n_d,n_d + 1,...} in the neglected terms is converging to zero, and thus neglecting these terms does only lead to small contributions to the approximation error.
- For any fixed time t and if the spectrum of A₁ is contained in the unit cycle, the matrices A₁^j, j ∈ {n_d, n_d + 1,...} in the neglected terms also converge to zero, thus leading to small errors.

The first countermeasure is included into the partitioning procedure in Section 3.1 Remark 2 by selecting sample points on the boundaries such that $j \cdot \Delta t < 1$ holds for all $j \in \{1, \dots, n_1\}$ in (9). The second countermeasure is established by ensuring that the largest singular value of A_1 is smaller than one, what can be guaranteed by observing the nonlinear matrix inequality:

$$A_1^T A_1 \prec I_{n_x}. \tag{11}$$

Note that larger numbers n_p of regions of the partition, in general, reduce the transition time from one boundary to the next, and thus lead to smaller approximation errors in the Taylor series expansion for a given order n_d (at the price of having to synthesize more pairs (A_i, b_i)). The condition (11) forces the eigenvalues of A_1 to be contained in the interior of the left half of the unit circle (since the contraction condition requires the real-part of the eigenvalues of A_1 to be negative in addition). Consequently, the convergence rate of (2) in the region P_1 is also bounded by 1, which can be counterproductive if the sample points to be tracked in F_1 encode that the state of the sampled limit cycle changes very differently in a certain region of the state space. As a result, the inclusion of (11) should be seen as an optional measure, or be replaced by a less conservative condition, such as $A_1^T A_1 \prec \beta I_{n_x}$ for some $\beta > 1$. The described countermeasures only affect the approximation quality without compromising the contraction property ensured by Lemma 1. A detailed analysis of the upper bound of the approximation error can be found in (Higham, 2009; Kenney and Laub, 1998).

The periodic signal u(t) can e.g. be chosen piecewise constant for $k \in \{0, 1, 2, ...\}$:

$$u(t) = \begin{cases} -1, \ t < [kT, (k + \frac{1}{2})T) \\ 1, \ t < [(k + \frac{1}{2})T, (k + 1)T). \end{cases}$$
 (12)

The integral part of (9) then leads to an analytic expression:

$$\begin{split} &\int_0^t e^{A_1(t-\tau)} (b_1 + Bu(\tau)) \ d\tau = \\ &\left\{ (e^{A_1t} - I_{n_x}) A_1^{-1} (b_1 - B) \text{ for } 0 \le t < \frac{1}{2}T \\ &(e^{A_1\frac{T}{2}} - I_{n_x}) A_1^{-1} (b_1 - B) + (e^{A_1(t-\frac{1}{2}T)} - I_{n_x}) A_1^{-1} (b_1 + B) \\ &\text{ for } \frac{1}{2}T \le t < T, \end{split} \right.$$

what is particularly beneficial for applying the previously discussed countermeasures in synthesis, see Section 3.4. Note that the matrix A_1 is always invertible, as the contractivity condition implies that A_1 must be Hurwitz.

3.4 Overall Optimization Problem

Given a partitioned state space according to Sec. 3.1 and a periodic signal u(t) of type (12), the optimization problem to synthesize the switching affine system (2) is defined as:

$$\min_{A_i, b_i, \alpha_i, i \in \{1, \dots, n_p\}, B, Q} \sum_{i=1}^{n_p} J_i$$
 (13)

s.t. for all $i \in \{1, ..., n_p\}$:

constraints (8)
$$\forall q \in \{1, \dots, n_x\},$$
 (14)

$$A_i^T Q + Q A_i \prec 0, \ Q \succ 0, \ B \neq 0, \tag{15}$$

$$A_i^T A_i \prec I_{n_x}$$
 (optional constraint), (16)

$$e^{A_i n_i \Delta t} \hat{x}_i + \int_0^{n_i \Delta t} e^{A_i (n_i \Delta t - \tau)} (b_i + Bu(\tau)) d\tau = \hat{x}_{i+1}. \quad (17)$$

In here, J_i is defined for each region in a similar way as J_1 in (9). This is a nonlinear optimization problem with in total $(n_P + 1)n_x^2 + (2n_P + 1)n_x$ variables. The cost functional minimized in (13) records the distance between each sample point in F and the point on the limit cycle of (2) at the same time. The constraints (14) and (15) guarantee that the resulting system (2) is contractive, while the optional constraint (16) aims at achieving a satisfying approximation by using the Taylor expansion for the matrix exponential function in (13) and (17). The last constraint aims at ensuring that the set of sample points \hat{x}_i , $i \in \{1, \ldots, n_P\}$ on the boundaries are reached by the limit cycle of (2). Otherwise, the minimization of (13) may only

force a transient trajectory of (2) to track the sample points in F, instead of the limit cycle of (2) (due to the approximation error of $e^{A_i t}$). In general, the optimization problem is not guaranteed to be feasible, but increasing the number n_p or choosing a different partition contributes to finding a feasible solution.

As an extension to account for transient behavior from arbitrary initial states to the limit cycle, an additional term can be included in (13) to minimize the deviation of the model dynamics from the sampled transient trajectories. Finally, it is worth mentioning that measurement noise (typically affecting the samples in F) is eliminated by the solution of (13) to (17) and assigning the model (2) to any of the regions P_i .

4 NUMERIC EXAMPLES

4.1 Illustrating Example in the Plane

To evaluate the performance of the proposed synthesis method, first an example of a set F of nineteen points in the plane is considered, as shown in Fig. 4 and Fig. 5 (marked by the solid black circles). The obtained period based on the sample set is T=1.4, which is also used for the periodic signal (12). In a first instance, the state space is partitioned by eight rays (solid blue lines) according to the rules provided in Section 3 with:

$$C_{1}=\begin{bmatrix}1 & -\frac{1}{4}\end{bmatrix}, C_{2}=\begin{bmatrix}1 & -2\end{bmatrix}, C_{3}=\begin{bmatrix}-1 & -2\end{bmatrix}, \\ C_{4}=\begin{bmatrix}-1 & -\frac{1}{4}\end{bmatrix}, C_{5}=\begin{bmatrix}-1 & \frac{1}{5}\end{bmatrix}, C_{6}=\begin{bmatrix}-1 & 3\end{bmatrix}, \\ C_{7}=\begin{bmatrix}1 & \frac{5}{2}\end{bmatrix}, C_{8}=\begin{bmatrix}1 & \frac{1}{6}\end{bmatrix}, d_{1}=\frac{1}{2}, d_{2}=-3, \\ d_{3}=-5, d_{4}=-\frac{3}{2}, d_{5}=-\frac{3}{5}, d_{6}=5, d_{7}=6, d_{8}=\frac{4}{3} \end{bmatrix}$$

using the center point $x_s = [1,2]^T$. The limit cycle of (2) obtained from solving the problem (13) with an order of $n_d = 4$ for the matrix exponential function is shown in Fig. 4. The shape of the limit cycle makes apparent that a small order n_d leads to considerable approximation errors. As a countermeasure, the order is increased to $n_d = 9$, for which the pairs (A_i, b_i) , $i \in \{1, ..., 8\}$ are obtained from solving the problem (13) (again with T = 1.4 in (12)). The resulting limit cycle is marked in black in Fig. 5.

The distance to the sampled points is much smaller, and trajectories from different initial points (in- and outside of the limit cycle) are simulated to demonstrate the stability and uniqueness of the limit cycle, see Fig. 5 and Fig. 6 (solid magenta, red and green). Note that the optional condition (16) was not used within this optimization, since the accuracy of the matrix exponential with $n_d = 9$ was acceptable.

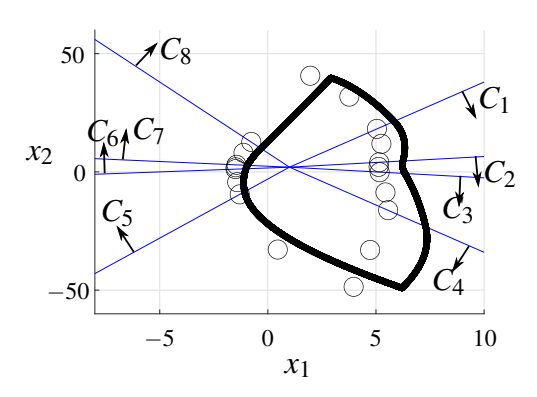


Figure 4: Sample points (black circles), switching boundaries in solid blue, and the limit cycle of the switching system with $n_d = 4$ in solid black.

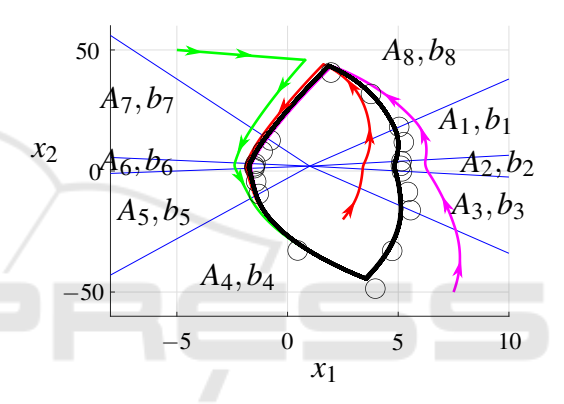


Figure 5: Sampled points (black circles) and switching boundaries in blue. The limit cycle is shown in black as well as trajectories from different initial points $x(0)=\begin{bmatrix}2.5 & -20\end{bmatrix}^T$ red, $x(0)=\begin{bmatrix}-5 & 50\end{bmatrix}^T$ green, and $x(0)=\begin{bmatrix}7.5 & -50\end{bmatrix}^T$ magenta.

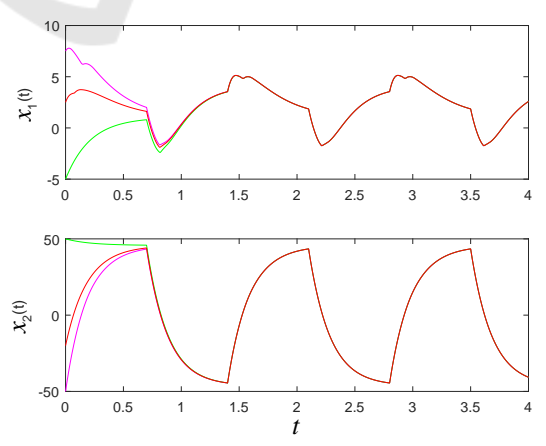


Figure 6: Convergence of $x_1(t)$ and $x_2(t)$ for different initial points $x(0) = \begin{bmatrix} 2.5 & -20 \end{bmatrix}^T$ red, $x(0) = \begin{bmatrix} -5 & 50 \end{bmatrix}^T$ green, and $x(0) = \begin{bmatrix} 7.5 & -50 \end{bmatrix}^T$ magenta.

4.2 Example in a 3D-Space

For an additional example within a 3-dimensional state space, consider the set of sample points illustrated in Fig. 7 (denoted by black circles). By applying the method described in Section 3.1 (case $n_x = 3$), and adhering to the requirement of the first countermeasure (transition times between sample points on adjacent boundaries are less than 1) leads to $n_p = 8$ subsets F_i to minimize the transition time between each pair of \hat{x}_i . Solving the optimization problem (4) and using the provided sample points as well as the center point $x_s = [1, 2, 0]^T$ provides the following result:

 $\Omega^* = \begin{bmatrix} -0.0115 & -0.0066 & 0.9999 \end{bmatrix}$, $\varepsilon^* = -0.0247$, which is shown as green plane in Fig. 7. The required line of intersection is given by $\Gamma := \{x \in \mathbb{R}^3 \mid x = x_s + \eta \Omega^*, \ \eta \in \mathbb{R} \}$, as marked by the solid blue line in Fig. 7. Since no point in F is contained in Γ , a unique plane containing both $(\Gamma \text{ and } \hat{x}_i)$ is determined for each sample point \hat{x}_i to:

$$C_{1} = \begin{bmatrix} 1 & -\frac{1}{4} & 0.0099 \end{bmatrix}, C_{2} = \begin{bmatrix} 1 & -2 & -0.0017 \end{bmatrix},$$

$$C_{3} = \begin{bmatrix} -1 & -2 & -0.0247 \end{bmatrix}, C_{4} = \begin{bmatrix} -1 & -\frac{1}{4} & -0.0132 \end{bmatrix},$$

$$C_{5} = \begin{bmatrix} -1 & \frac{1}{5} & -0.0102 \end{bmatrix}, C_{6} = \begin{bmatrix} -1 & 3 & 0.0083 \end{bmatrix},$$

$$C_{7} = \begin{bmatrix} 1 & \frac{5}{2} & 0.0280 \end{bmatrix}, C_{8} = \begin{bmatrix} 1 & \frac{1}{6} & 0.0126 \end{bmatrix}, d_{1} = 0.5, d_{2} = -3$$

$$d_{3} = -5, d_{4} = -1.5, d_{5} = -0.6, d_{6} = 5, d_{7} = 6, d_{8} = 1.33,$$

see the solid blue planes in Fig. 7. The resulting limit cycle obtained from solving the optimization problem in Section 3.4 is marked in black in Fig. 7. The distance to the sampling points is once again acceptable,

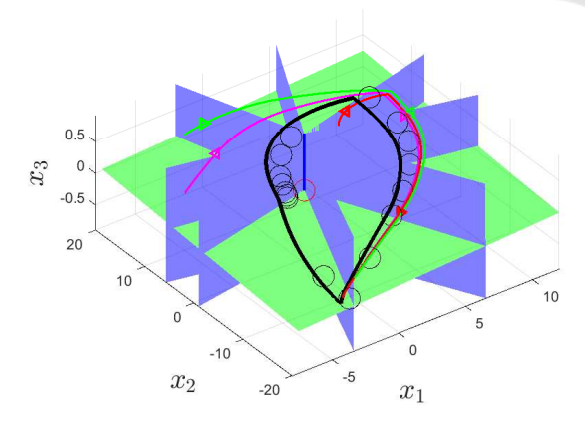


Figure 7: Sampled points (black circles), green plane with minimum distance to the sampled points including x_s (red circle), the line of intersection Γ as solid blue line and boundaries shown as planes in blue, while the limit cycle is marked in black and the trajectories from different initial points $x(0) = \begin{bmatrix} 6.5 & 10 & 0.1 \end{bmatrix}^T \text{ red}, x(0) = \begin{bmatrix} -1.9 & 18.5 & 0.18 \end{bmatrix}^T \text{ green, and } x(0) = \begin{bmatrix} -5 & 10 & 0 \end{bmatrix}^T \text{ magenta.}$

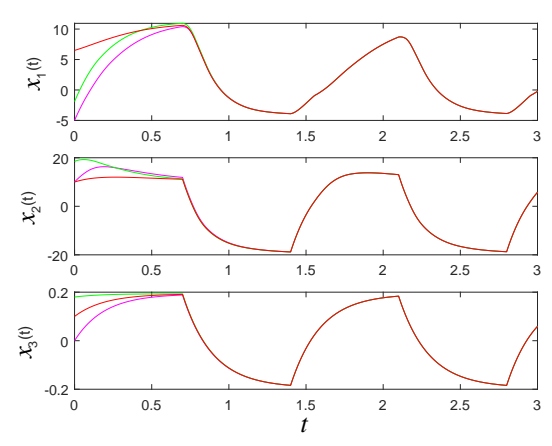


Figure 8: Convergence of $x_1(t)$, $x_2(t)$, $x_3(t)$ for different initial points $x(0) = \begin{bmatrix} 6.5 & 10 & 0.1 \end{bmatrix}^T$ red, $x(0) = \begin{bmatrix} -1.9 & 18.5 & 0.18 \end{bmatrix}^T$ green, and $x(0) = \begin{bmatrix} -5 & 10 & 0 \end{bmatrix}^T$ magenta.

even though all dimensions are on significantly different scales, which underscores the approximation quality of the approach. Trajectories from different initial points again demonstrate the convergence to the unique limit cycle, see Fig. 7 and Fig. 8 with trajectories in magenta, red, and green.

5 CONCLUSIONS

This work has introduced a method for approximating periodic behavior of nonlinear dynamic systems not restricted to the planar case. Based on suitable sampling of the limit cycle of the nonlinear dynamics, switched affine systems with exogenous inputs are used for approximation, while the approach preserves essential limit cycle properties including stability and uniqueness. Unlike previously available methods, the work here provides constructive rules to partition the state space and synthesize the dynamics by optimization, such that the limit cycle of the switching affine system matches the sample points of the nonlinear data generator in an optimized sense. By using the notion of contractivity, the constructed limit cycle is ensured to be globally stable. Although the introduced conditions generate a non-convex and nonlinear optimization problem, they simultaneously ensure a smooth limit cycle, a behavior frequently observed in real-world systems. While solvability of the optimization problem cannot be guaranteed, any solution found under these conditions will be convergent.

It should be noted that the use of a center point in which all boundaries intersect is particularly suitable if the sample points have a relatively even distribution around an interior region in \mathbb{R}^{n_x} .

Future work aims at investigating schemes of partitioning without a common center point, and the coupling of several oscillators of the proposed type.

ACKNOWLEDGEMENTS

Partial financial support by the German Research Foundation (DFG) through the Research Training Group *Biological Clocks on Multiple Time Scales* (GRK 2749/1) is gratefully acknowledged.

REFERENCES

- Atherton, D. and Dorrah, H. (1980). A survey on non-linear oscillations. *International Journal of Control*, 31(6):1041–1105.
- Bernardo, M., Budd, C., Champneys, A. R., and Kowalczyk, P. (2008). *Piecewise-smooth dynamical systems: theory and applications*, volume 163. Springer Science & Business Media.
- Coll, B., Gasull, A., and Prohens, R. (2001). Degenerate hopf bifurcations in discontinuous planar systems. *Journal of mathematical analysis and applications*, 253(2):671–690.
- Demidovich, B. P. (1967). Lectures on stability theory.
- Dörfler, F. and Bullo, F. (2014). Synchronization in complex networks of phase oscillators: A survey. *Automatica*, pages 1539–1564.
- Freire, E., Ponce, E., Rodrigo, F., and Torres, F. (1998). Bifurcation sets of continuous piecewise linear systems with two zones. *International Journal of Bifurcation and Chaos*, 8(11):2073–2097.
- Gaiko, V. A. (2011). Multiple limit cycle bifurcations of the fitzhugh–nagumo neuronal model. Nonlinear Analysis: Theory, Methods & Applications, 74(18):7532– 7542
- Gonze, D. and Ruoff, P. (2021). The goodwin oscillator and its legacy. *Acta Biotheoretica*, 69(4):857–874.
- Hanke, N., Liu, Z., and Stursberg, O. (2024). Approximation of limit cycles by using planar switching affine systems with guarantees for uniqueness and stability. In *European Control Conference*, pages 1460–1465.
- Hanke, N., Liu, Z., and Stursberg, O. (2025). Approximation of planar periodic behavior from data with stability guarantees using switching affine systems. In American Control Conference, pages 1944–1949.
- Hanke, N. and Stursberg, O. (2023). On the design of limit cycles of planar switching affine systems. In *European Control Conference*, pages 2251–2256.
- Higham, N. J. (2009). The scaling and squaring method for the matrix exponential revisited. *SIAM review*, 51(4):747–764.
- Joshi, S. K., Sen, S., and Kar, I. N. (2016). Synchronization of coupled oscillator dynamics. *IFAC-PapersOnLine*, 49(1):320–325.

- Kai, T. and Masuda, R. (2012). Limit cycle synthesis of multi-modal and 2-dimensional piecewise affine systems. *Mathematical and Computer Modelling*, 55(3-4):505–516.
- Kenney, C. S. and Laub, A. J. (1998). A schur–fréchet algorithm for computing the logarithm and exponential of a matrix. *SIAM journal on matrix analysis and applications*, 19(3):640–663.
- Kudryashov, N. A. (2021). The generalized duffing oscillator. Communications in Nonlinear Science and Numerical Simulation, 93:105526.
- Kuramoto, Y. (2005). Self-entrainment of a population of coupled non-linear oscillators. In *International symposium on mathematical problems in theoretical physics. Kyoto University, Japan*, pages 420–422. Springer.
- Lauer, F., Bloch, G., and Vidal, R. (2011). A continuous optimization framework for hybrid system identification. *Automatica*, 47(3):608–613.
- Llibre, J., Ponce, E., and Torres, F. (2008). On the existence and uniqueness of limit cycles in liénard differential equations allowing discontinuities. *Nonlinearity*, 21(9):2121.
- Lum, R. and Chua, L. O. (1991). Global properties of continuous piecewise linear vector fields. part i: Simplest case in \mathbb{R}^2 . *International journal of circuit theory and applications*, 19(3):251–307.
- Mirollo, R. E. and Strogatz, S. H. (1990). Synchronization of pulse-coupled biological oscillators. *SIAM Journal on Applied Mathematics*, 50(6):1645–1662.
- Paoletti, S., Juloski, A. L., Ferrari-Trecate, G., and Vidal, R. (2007). Identification of hybrid systems a tutorial. *European journal of control*, 13(2-3):242–260.
- Pavlov, A., Pogromsky, A., Van De Wouw, N., and Nijmeijer, H. (2007). On convergence properties of piecewise affine systems. *International Journal of Control*, 80(8):1233–1247.
- Peterchev, A. V. and Sanders, S. R. (2003). Quantization resolution and limit cycling in digitally controlled pwm converters. *IEEE Transactions on Power Electronics*, 18(1):301–308.
- Teplinsky, A. and Feely, O. (2008). Limit cycles in a mems oscillator. *IEEE Transactions on Circuits and Systems II: Express Briefs*, 55(9):882–886.
- Werckenthin, A., Huber, J., Arnold, T., Koziarek, S., Plath, M. J., Plath, J. A., Stursberg, O., Herzel, H., and Stengl, M. (2020). Neither per, nor tim1, nor cry2 alone are essential components of the molecular circadian clockwork in the madeira cockroach. *PLoS One*, 15(8):e0235930.
- Xu, Y. and Luo, A. C. (2019). Frequency-amplitude characteristics of periodic motions in a periodically forced van der pol oscillator. *The European Physical Journal Special Topics*, 228(9):1839–1854.